BMC Oral Health

RESEARCH

Open Access

Effect of zinc oxide/graphene oxide nanocomposites on the cytotoxicity, antibacterial and mechanical properties of polymethyl methacrylate

Shaofan Ruan[1], Yanzong Zhao[1], Rui Chen[1*], Jie Ma[1], Yian Guan[1], Jianqiang Ma[1] and Liling Ren[1*]

Abstract

Background Enhancing the antibacterial properties of polymethyl methacrylate (PMMA) dental resins is crucial in preventing secondary infections following dental procedures. Despite the necessity for such improvement, a universally applicable method for augmenting the antibacterial properties of PMMA without compromising its mechanical properties and cytotoxicity remains elusive. Consequently, this study aims to address the aforementioned challenges by developing and implementing a composite material known as zinc oxide/graphene oxide (ZnO/GO) nanocomposites, to modify the PMMA.

Methods ZnO/GO nanocomposites were successfully synthesized by a one-step procedure and fully characterized by TEM, EDS, FTIR and XRD. Then the physical and mechanical properties of PMMA modified by ZnO/GO nanocomposites were evaluated through water absorption and solubility test, contact angle test, three-point bending tests, and compression test. Furthermore, the biological properties of the modified PMMA were evaluated by direct microscopic colony count method, crystal violet staining and CCK-8.

Results The results revealed that ZnO/GO nanocomposites were successfully constructed. When the concentration of nanocomposites in PMMA was 0.2 wt. %, the flexural strength of the resin was increased by 23.4%, the compressive strength was increased by 31.1%, and the number of bacterial colonies was reduced by 60.33%. Meanwhile, It was found that the aging of the resin did not affect its antibacterial properties, and CCK-8 revealed that the modified PMMA had no cytotoxicity.

Conclusion ZnO/GO nanocomposites effectively improved the antibacterial properties of PMMA. Moreover, the mechanical properties of the resin were improved by adding ZnO/GO nanocomposites at a lower range of concentrations.

Keywords Zinc oxide/Graphene oxide, Polymethyl methacrylate, Antibacterial property, Cytotoxicity

*Correspondence:
Rui Chen
chenr14@lzu.edu.cn
Liling Ren
renlil@lzu.edu.cn
[1] School and Hospital of Stomatology, Lanzhou University, 222 Tianshui South Road, Lanzhou, Gansu 730000, China

Background

Polymethyl methacrylate (PMMA) has been widely used in clinical work, particularly in the fields of orthodontics and prosthodontics, owing to its numerous benefits such as excellent biocompatibility, convenient processing, great aesthetics, and high-cost performance [1–3].However, the insufficient antimicrobial properties of PMMA

make it easy to deposit of the dental plaque biofilm in the oral environment during use [4, 5], resulting in dental caries, mucosal infections, periodontal diseases and even systemic disease such as cardiovascular disease and diabetes mellitus [6–10], which limits the widespread clinical use of PMMA.

Usually, antibiotics and cleaning are the most effective and conventional methods to address the aforementioned issues. However, the long-term use of antibiotics has negative impacts on physical health and can also increase the rates of antibiotic resistance. Moreover cleaning methods such as manual washing, disinfectant soaking, and ultrasonic cleaning may accelerate unwanted wear down of materials and cleaning methods are merely realizable for removable dental applications [11, 12].

Compared to the antibiotics and cleaning methods, the novel approach of antibacterial modification of PMMA with different fillers can prevent bacterial from adhering to the surface of the resin [13–18], and significantly lessen the dental plaque biofilm on the surface of the resin. Among the existing researches, commonly used filler materials include organic materials such as ethylenediaminetetraacetic acid (EDTA) [14], dimethylaminohexadecyl methacrylate (DMAHDM) [15], and inorganic nanoparticles such as Au [16, 17], Ag [18], TiO_2 [13]. The addition of fillers improves the antimicrobial properties of PMMA to some extent, but often has a negative impact on the mechanical properties (EDTA, Au, Ag, TiO_2) or biocompatibility (DMAHDM) of PMMA. Obviously, all these approaches have inevitable drawbacks that limit the clinical application of PMMA. Therefore, a novel strategy to solve the aforementioned problems is urgently required.

Zinc oxide nanoparticles (ZnO NPs) have excellent biocompatibility and broad-spectrum antimicrobial activity against both gram-positive and gram-negative bacteria [19]. At present, the release of Zn^{2+} ions and generation of reactive oxygen species (ROS) are considered as the main antimicrobial mechanisms of ZnO NPs [20, 21]. However, ZnO NPs have tendency to agglomerate, thus limiting the antibacterial activities [22]. Therefore, avoiding the aggregation of ZnO NPs is the key to its antibacterial effect.

The introduction of graphene oxide (GO) has the potential to solve the agglomeration of ZnO NPs. The main reason is that the oxygen-containing functional groups on the surface of ZnO NPs could serve as bonding sites for metals and metal oxides. Therefore, GO, as the dispersant, can prevent the self-agglomeration of ZnO NPs [23, 24]. Moreover, GO nanosheets displays properties such as a high surface area, good mechanical strength and chemical stability. Several studies have suggested GO could strengthen mechanical performance of PMMA [25, 26], such as Cahyanto et al. [27] found that GO significantly improved the fatigue resistance and service life of PMMA.

In this study, PMMA was modified by adding ZnO/GO nanocomposites with different concentrations, and the cytotoxicity, mechanical and antimicrobial properties of the modified resin were comprehensively evaluated in vitro.

Methods

Preparation of the ZnO/GO nanocomposite

$Zn(CH_3COO)_2{\cdot}2H_2O$ (0.32 g) (Solarbio, Beijing, China) was dissolved in 30 mL anhydrous ethanol (Damao Chemical Reagent Factory, Tianjin, China) and the solution was stirred at 80 y for 15 min, then cooled down to 40 ℃. $LiOH{\cdot}H_2O$ (0.12 g) (Solarbio, Beijing, China) was dissolved in 12 mL anhydrous ethanol, then 20 mL GO (2 mg/mL) (Solarbio, Beijing, China) was added in, both solutions were mixed by vigorous stirring. After that, the mixture was added into the zinc acetate solution under consistent stirring at room temperature for 1 h. The mixture was set in n-hexane overnight at 4 ℃. The precipitates were collected by centrifugation, then washed with ethanol and deionized water, drying at 60 °C for 12 h in a vacuum oven.

Characterization of the ZnO/GO nanocomposites

The morphology of the ZnO/GO nanocomposite was characterized by transmission electron microscopy (TEM, JEM-2100F, Joel, Tokyo, Japan). The composition of the ZnO/GO nanocomposites was checked by X-ray diffractometer (XRD, Smart APEX II, BRUKER, Germany) and Fourier transform infrared (FTIR, Nicolet, NEXUS 670, American) spectroscopy using the KBr method.

Modifying the PMMA with ZnO/GO nanocomposites

The experimental groups were established based on the varying mass ratios between PMMA powders (Xinshiji, Shanghai, China) and ZnO/GO nanocomposite. 0 wt. % was the negative control group, 0.1 wt. %, 0.2 wt. %, 0.3 wt. % and 0.4 wt. % were all experimental groups. For example, the 0.2 wt. % group contains 10 g of PMMA powder and 0.2 g of ZnO/GO nanocomposite.

Five identical-mass pieces of the ZnO/GO nanocomposite were dispersed in deionized water via ultrasonication, this was followed by the addition of correctly proportioned PMMA powder, mixed for 24 h, and dried. The specimens were then produced using the manufacturer's specified powder-liquid ratio (22 g/10 ± 0.5 mL) (Fig.1)

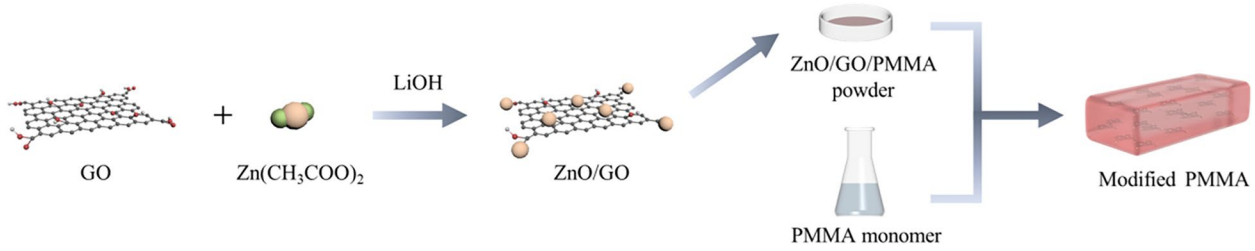

Fig. 1 Schematic of the PMMA resin modified with ZnO/GO nanocomposites

Flexural strength

In accordance with the ISO 20795–1 international standard, specimens (65 mm long × 10 mm wide × 3.3 mm thick, $n = 3$) were made for the purpose of conducting three-point bending test. A total of five groups of specimens were prepared. Following a 24 h immersion in deionized water at a temperature of 37 °C, the specimens underwent evaluation using a universal mechanical testing machine (R Controller, Testresources, Shakopee, MN, USA) at a rate of 0.50 mm/min until the specimens experienced fracture (Fig. 3A). The flexural strength (σ, MPa) of each specimen was calculated by the following formula.

$$\sigma = \frac{3FL}{2BH^2} \quad (1)$$

F is the maximum load applied to the specimen at the point of fracture, L is the distance between the two supports (45 mm), B is the width (mm), and H is the thickness (mm) between the two surfaces of the specimen.

Compressive strength

The compressive strength of PMMA is tested in line with the ISO 20795–1 standard of the International Organization for Standardization. The specimens (4 mm diameter × 6 mm height, $n = 3$) were made in cylindrical metal molds. Following a 24 h period of storage in deionized water at a temperature of 37 °C, the compressive strength was evaluated using a universal mechanical testing machine operating at a rate of 0.50 mm/min.

The compressive strength (C, MPa) of each nanocomposite specimen was calculated by the following formula.

$$C = \frac{4p}{\pi d^2} \quad (2)$$

p is the maximum applied load (N) measured, and d is the diameter of the specimen (mm).

Cross-sectional observation

The specimens were collected after flexural strength test and then sprayed with gold using an injection current of 10 mA for 60 s by a sprayer (108auto, Ted Pella, Redding, CA, USA). Scanning electron microscopy (SEM, jsm-5600lv, Joel, Tokyo, Japan) was used to explore the features of the fractured surfaces at 1,000 × magnifications.

Water absorption and solubility

Cylindrical specimen with dimensions (4 mm diameter × 6 mm height, $n = 3$) were made for the tests. The weight of specimen was measured on the analytical balance (Mettler Toledo ME204, Columbus, OH, USA). The 24 h drying cycle was iterated until the initial dry weight (W_0) was achieved, with a mass change of less than ± 0.001 mg. The specimens were immersed in 15 ml of deionized water which refreshed daily. After immersion for durations of 7, 14, and 28 days, the specimens were wiped with absorbent paper for 3 s and shaken in the air for 10 s, then weighed immediately, which was recorded as wet weight (W_1). At the end of the immersion period, the specimens were dried as previously described until the specimens reached a constant mass (W_2). The water absorption and solubility were calculated by the following formula.

$$\text{Water absorption} = (W_1 - W_2)/W_2 \times 100\% \quad (3)$$

$$\text{Solubility} = (W_0 - W_2)/W_0 \times 100\% \quad (4)$$

Antibacterial activity

S. mutans (ATCC® 700,610, Huayueyang Bio, Shenzhen, China) was incubated for 6 h in Luria–Bertani (LB) (Solarbio, Beijing, China, L1010) at 37 °C in a 5% CO_2 incubator, the bacterial suspension was diluted with fresh LB for further use. After that, the aged and non-aged specimens (10 mm diameter × 1.5 mm height, $n = 3$) were made. To obtain aged specimens, the modified PMMA was immersed in fresh deionized water that was replaced daily at 37 °C for 28 days. All the specimens were sterilized under ultraviolet light via a UV irradiator (HFsafe-1200LC, Likang, Shanghai, China) 1 h.

Each specimen was put in a well of 24-well plate, then 10 μL S. mutans suspension (10^6 colony-forming unit (CFU) / ml) was vertically dropped on the center of specimen's surface. Subsequently, surfaces were carefully covered with films in a bid to form even and thin biofilms. Then, the well plates were cultured in an incubator at 37 °C with relative humidity greater than 90% for 24 h. After that, the film and surface were washed by 1 mL LB medium, respectively. The obtained solutions were diluted 20 times and 100 μL of that was dropped on an LB ager plate, then incubated at 37 °C for 24 h. Finally, bacterial colonies on the plates were photographed and counted by Image-J 2x (Rawak Software, Stuttgart, Germany). All experiments were performed in triplicate. Blank controls were used with Teflon membranes.

The antibacterial rate was calculated as follows:

$$R\,(\%) = [(B - C)/B] \times 100\% \quad (5)$$

R is the antibacterial rate; B is the mean colony-forming unit (CFU) value of the blank control group; C is the mean CFU value of the modified resin group.

The specimens were treated in the same manner as described above. After 24 h of incubation at 37 °C, the specimens were washed with phosphate buffer saline (PBS) to remove any unadhered bacteria. Then, for SEM observations, the bacteria on the specimens was fixed in 2.5% glutaraldehyde (Sigma-Aldrich, American) and dehydrated with graded ethanol.

Following that, the crystal violet semi-quantitative staining method was used to determine biofilm forming ability. bacterial suspensions (10 μL) at the logarithmic growth phase were added to 990 μL LB medium in the 24-well plate. PMMA resin specimens containing different concentrations of ZnO/GO nanocomposites were immersed in the culture medium and cultured in a constant temperature incubator at 37 °C for 48 h. Next, the specimens were transferred to a new 24-well plate, and gently rinsed three times with PBS buffer to remove non-adherent bacteria. After that, the surface of the specimen was stained with 1% crystal violet solution (Aladding, China, C110703) at 37 °C for 5 min. Then, the 24-well plate was rinsed with running deionized water for 5 min. Subsequently, the surface of the specimen was washed with 1 mL of 50% glacial acetic acid solution. 100 μL eluted was pipetted into each well of 96 well plate, and the absorbance was measured at 575 nm. At least three parallel specimens of each group were measured.

Cytotoxicity assay

The cytotoxicity of PMMA was evaluated by assaying the viability of fibroblasts (L-929 cell line, Shanghai Cell Bank, Chinese Academy of Sciences) in vitro. Before use in cell culture experiments, the specimens (d × h = 10 mm × 1.5 mm, $n = 3$) were thoroughly sterilized by UV irradiation and immersed in deionized water for 24 h.

Firstly, the specimens were immersed in dulbecco's modified eagle medium (DMEM) without fetal bovine serum (FBS) at 37 ℃ for 48 h, and the corresponding DMEM (Yuanpei, Shanghai, China, L10KJ) was collected for cell culture experiments. Next, the cells suspension was seeded into 96-well plate (5×10^3 cells per well) and incubated for 24 h. After that, the medium was replaced with the previously collected H-DMEM, then incubated for 24, 48 and 72 h. Finally, 10 μL CCK-8 (Servicebio, Wuhan, China, G4103) was added and incubated for a further 3 h, before the absorbance was measured at 450 nm and the cell viability calculated.

Statistical analysis

The results were analyzed by SPSS software version 27 (SPSS Ins., Chicago III., USA). Descriptive statistics (mean and standard deviation) were used to describe the data, Shapiro–Wilk test was used to assess normality of the data distribution, and One-way analysis of variance (ANOVA) and Waller–Duncan K-ratio t-test was used to compare the groups. The differences were considered statistically significant at $p < 0.05$. In all figures, the number of asterisks is associated with the p-value (* $p < 0.05$, ** $p < 0.01$, *** $p < 0.001$), and the error bars represent standard deviations (SD), which the geometric symbols on represent the experimental values for each specimen tested.

Results

Characterization of the ZnO/GO nanocomposites

The effective combination of GO and ZnO NPs is the fundamental prerequisite for ZnO/GO nanocomposites to enhance the mechanical and antibacterial properties of PMMA. TEM and EDS mapping technique showed that the ZnO/GO nanocomposites were successfully synthesized. It can be found that ZnO NPs were evenly distributed on the GO sheet (Fig. 2A), and the diffraction streaks confirm that the lattice spacing was 0.28 nm (shown by the white arrow), which was consistent with the characteristics of ZnO nanocrystals. In addition, EDS mapping analysis showed that scattered Zn elements distributed throughout the GO sheet (Fig. 2B), which indicated the presence of ZnO NPs on GO. To further confirm the formation of ZnO/GO nanocomposites, the XRD patterns of the ZnO/GO nanocomposites were recorded (Fig. 2C). In the XRD patterns of the ZnO/GO nanocomposites exhibited a standard GO diffraction peak at $2\theta = 10.8°$ and prominent ZnO diffraction peaks at $2\theta = 31.4°$, 35.9°, 47.4°and 56.3°, which corroborated the successful combination of the ZnO NPs with the GO.

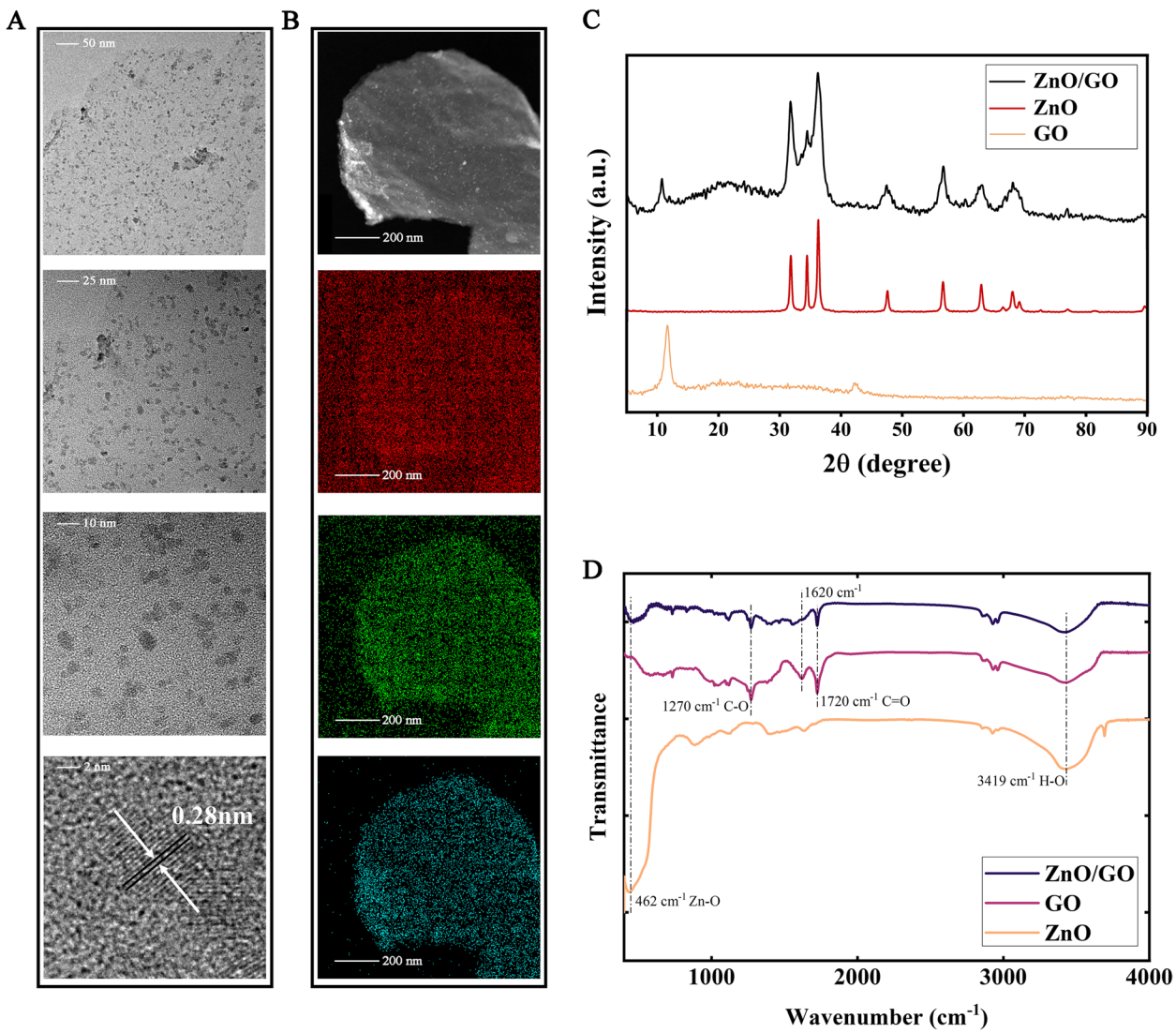

Fig. 2 TEM micrograph for ZnO/GO (**A**), white markers are crystal plane spacing of ZnO, the inset of (**B**) is HAADF-STEN image of ZnO/GO and EDS mapping analysis of C, O, and Zn, from top to bottom, XRD pattern (**C**) and FTIR spectra (**D**) for ZnO/GO

In order to further analyze the functional groups on the surface of the ZnO/GO nanocomposites, FTIR was performed (Fig. 2D). In all FTIR plots, the absorption peak at 3149 cm^{-1} was attributed to the vibrations of the H–O bond. The detected peak at 462 cm^{-1} could be assigned to the vibrations of the Zn = O bonds in the ZnO and nanocomposites, this indicated that the ZnO/GO nanocomposites do indeed contain ZnO. And, the absorption peaks at 1270 cm^{-1} and 1720 cm^{-1} respectively indicated C-O stretch and C = O stretch of GO [28, 29], the absorption peak at 1620 cm^{-1} could be attributed to the Reduced Graphene Oxide (RGO) [30].

All of the above had proved that the ZnO/GO nanocomposites were successfully synthesized with GO and ZnO NPs.

Physical properties of PMMA resin modified by ZnO/GO nanocomposites

Flexural and compressive strengths are key indicators for evaluating the mechanical properties of materials. First, the flexural resistance of the PMMA resin was measured and denoted with flexural strength. The results showed that the flexural strength of the PMMA resin modified by ZnO/GO nanocomposites was increased compared

with the control group, when the concentration of ZnO/GO was 0.1wt. %, 0.2 wt. %, and 0.3 wt. %, especially this effect was more pronounced when the nanocomposites content was 0.2 wt. % (Fig. 3B).

Similarly, the compressive strength of the modified PMMA was increased, when the concentration of ZnO/GO was 0.1wt. %, 0.2 wt. %, and 0.3 wt. %. And the compression strength of the 0.2 wt. % and 0.3 wt. % groups were greater than 100 MPa (Fig. 3C). However, it needs to be emphasized that the increment in flexural and compressive strength decreased, when the nanocomposites content was 0.3 wt. % and 0.4 wt. %. In addition, there was no significant difference in the both strength between 0.4 wt. % groups and control groups. To better understand the microscopic mechanism, we examined the cross-sections of the specimens by SEM. It was found that there were variable number of microcracks on the cross-sectional surface of specimens (Fig. 3D). With increasing concentrations of ZnO/GO nanocomposites, the number of microcracks gradually decreased. However, with the further increase the concentration of the nanocomposites, the number of microcracks increased again.

In addition, water absorption and solubility affect the dimensional stability and mechanical properties of PMMA [31, 32]. As can be seen from the Fig. 3E-F, with the extension of the immersion time, the water absorption and solubility of the resin increased, and five groups did not show any significant difference on the 7th, 14th and 28th day of the experiment.

The magnitude of the water contact angle was inversely proportional to the hydrophilicity. As shown in Fig. 4A-B, the contact angle decreased with increasing the content of ZnO/GO nanocomposites, and the contact angle in all groups decreased gradually over time, indicating that all of the resin groups showed high hydrophilicity, and the hydrophilicity of the specimens increased with increasing content of nanocomposites.

Antibacterial activity

In this study, we evaluated the effects of ZnO/GO nanocomposites on the antibacterial of PMMA resin. The results showed that the number of colonies on the surface of PMMA resin was significantly reduced after modified by ZnO/GO nanocomposites. When the concentrations of ZnO/GO nanocomposites were 0.2 wt. %, 0.3 wt. % and 0.4 wt. %, the number of colonies on the surface of resin was decrease by 60.33%, 82.68% and 92.21%, respectively (Fig. 5A, 5B). At the same time, we found that there was no significant difference in the number of colonies on the resin surface between the aged and non-aged groups, which may be owed to the capacity of sustained release of antibacterial ions with the ZnO/GO nanocomposites system [23].

Additionally, the results of the crystal violet semi-quantitative staining showed that the plaque biofilm deposited on the surface of the resin was significantly reduced after the resin was modified by ZnO/GO nanocomposites, especially when the concentration of nanocomposites was greater than 0.2 wt. %, this change was very significant (Fig. 5C). We also found that the morphology of S. mutans on the surface of the modified resin was changed, manifested as the disappearance of the normal oval profile, irregular bacterial morphology and a decrease in the bacteria in the in the number of bacteria during division (Fig. 5D) (shown in red circle).

Cytotoxicity assay

Finally, CCK-8 assay was used to evaluate the effect of PMMA resin on the viability of L929 cells. The results showed that the cell viability decreased slightly with time in all groups, but there was no significant difference between the groups (Fig. 6). This suggested that the modified resin still had no cytotoxicity.

Discussion

Plaque biofilms are easily formed on PMMA surfaces in the oral environment, which can lead to dental caries, denture stomatitis and other oral mucosa lesions. Therefore, the application of PMMA in the oral cavity is substantially limited due to its inadequate antibacterial properties. Numerous researches attempted to enhance the antimicrobial properties of PMMA, but they often negatively affect the cytotoxicity and mechanical properties of the resin. The objective of this study was to enhance the antibacterial properties of PMMA, ensuring the cytotoxicity and mechanical properties of material in the meantime.

We first synthesized ZnO/GO nanocomposite and characterized the products by TEM, EDS Mapping, XRD and FTIR techniques. The characterization results validated the effective synthesis of ZnO/GO nanocomposites in terms of microstructure and surface topography. Furthermore, the mechanical properties of the modified resin were studied by the compressivetest and the three-point bending test. The results showed that the flexural strength and compressive strength of the PMMA were significantly improved when the concentration of the ZnO/GO nanocomposite reached 0.2 wt. %, which was considerably superior than ISO 20795–1 standard. This can be explained by the uniform dispersion of ZnO/GO nanocomposite particles throughout the PMMA resin and the good bonding strength between the nanocomposite and matrix. The nanoparticles were capable of filling in voids surrounding the

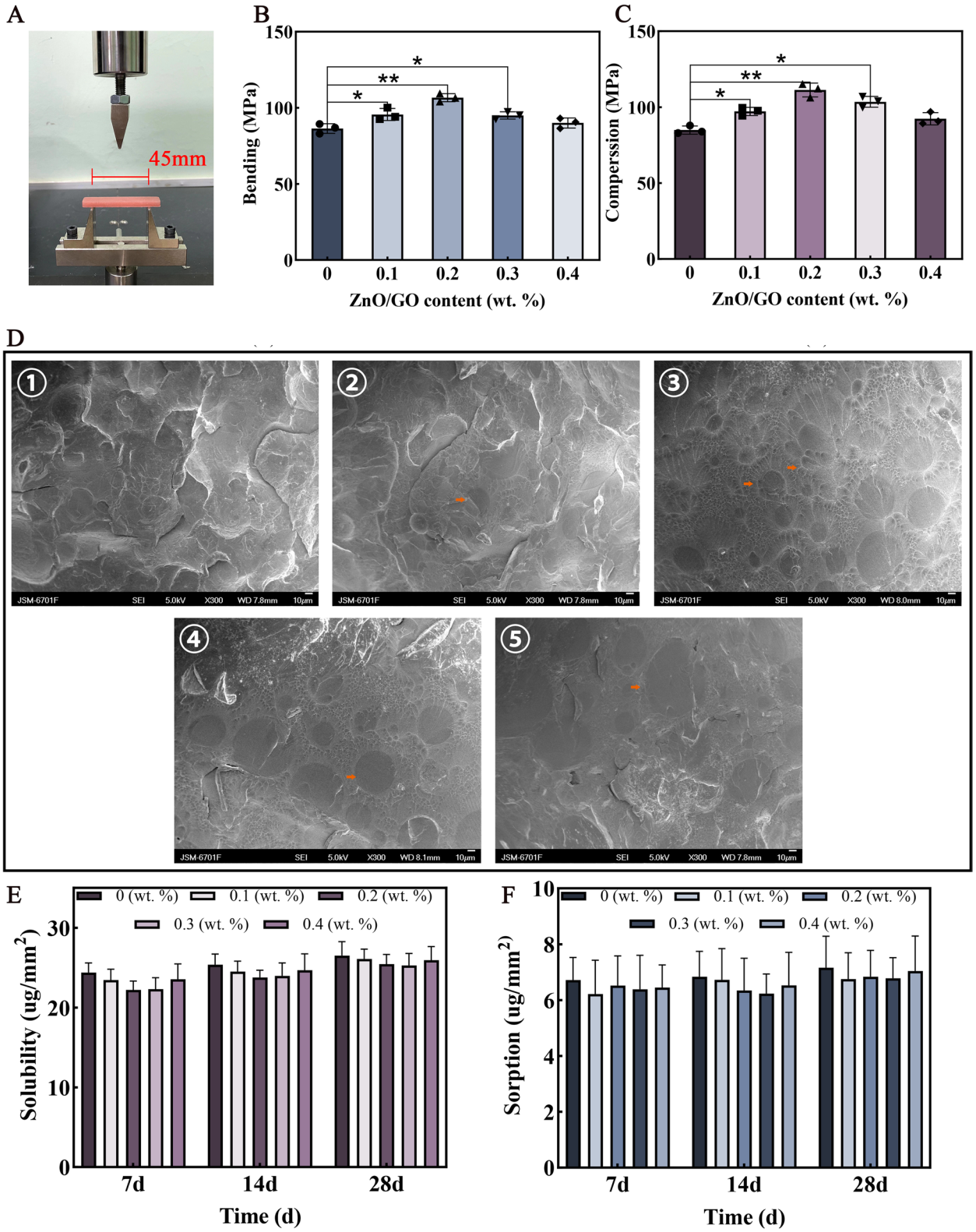

Fig. 3 Photograph of the three-bending test (**A**), Fracture strength (**B**) and Compressive strength (**C**) of the modified PMMA, SEM images of fractured specimens (**D**, ①-⑤ show the 0 wt.%, 0.1 wt.%, 0.2 wt.%, 0.3 wt.%, 0.4 wt.% of ZnO/GO respectively), the orange arrow indicate that the oval structures discovered on the surface of the modified PMMA, Solubility (**E**) and Water absorption (**F**) value of the modified PMMA ($n = 3$, * $p < 0.05$, ** $p < 0.01$, *** $p < 0.001$)

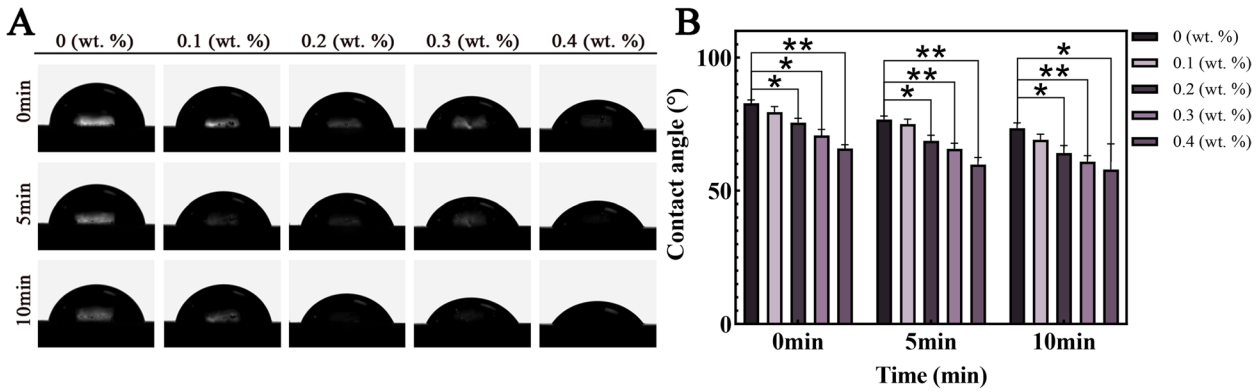

Fig. 4 Contact angle (**A**, **B**) of the modified PMMA ($n=3$, * $p<0.05$, ** $p<0.01$, *** $p<0.001$)

polymer chains, and when the resins were subjected to external stress, the load could be transferred from the matrix material to the nanoparticles. This prevented the propagation of cracks due to the strong interfacial interactions between the nanoparticles and the resin matrix. Evidence of the intrinsic reinforcement can be also seen in cross-sectional SEM images. When doped with 0.2 wt. % ZnO/GO, the resin had the best mechanical properties and least microcracks. However, when the concentration of the nanocomposite within the polymer resin was further increased, the mechanical properties decreased due to nanoparticle agglomeration, leading to discontinuities in the resin matrix. In the presence of multiple agglomerates, the stress is concentrated at each agglomeration site, resulting in expansion of microcracks [33].

Notably, oval structures (shown by arrows) were discovered on the surface of the resin containing doped nanocomposites at concentrations of 0.1 wt. %, 0.2 wt. %, 0.3 wt. %, and 0.4 wt. % groups (Fig. 3D ②-⑤). This could be due to GO scavenging part of the free radicals, resulting in incomplete polymerization of PMMA, leading to a portion of the powder not being completely polymerized [34]. However, it did not negatively affect the physical and mechanical properties of the modified PMMA significantly.

Water absorption and solubility were emplored to evaluate the stability of ZnO/GO nanoparticles. Water sorption by acrylic resins can affect the dimensional stability and can lead to failure of the prosthesis [31, 32, 35]. Conversely, the high solubility of acrylic resins might contribute to the existence of unreacted monomers, which have negative effects on oral tissues [36]. The modified PMMA fulfilled the standard that the water absorption and solubility of this type of PMMA should not be higher than 32 μg/mm^3 and 8 μg/mm^3, as recommended by ISO 20795–1. In addition, the modified PMMA exhibited a modest decrease in solubility and water absorption. This can be attributed to the nanoparticles' capacity to occupy the empty spaces within the polymer resin, resulting in a more compact and firm structure with reduced porosity.

The water contact angle is commonly used to evaluate the hydrophilicity of a material surface, with a smaller water contact angle indicating a higher degree of hydrophilicity. In this study, with the doping ratio of ZnO/GO increased, the hydrophilicity of the PMMA resin surface also increased, which may be connected to the significant amount of negative charge stored on the surface of GO [37]. It had been shown that the more hydrophilic the PMMA resin is, the stronger its adsorption to the oral mucosa, hence preventing the dislocations of the PMMA resin [38]. Additionally, the hydrophilicity of the material's surface influences microbial deposition [39]. Lazarin et al. [40] demonstrated candida albicans, the fungus that causes denture stomatitis, cannot adhere to a hydrophilic resin surface. Therefore, increasing hydrophilicity of the PMMA resins not only improve retention but also help to reduce microbial adherence.

The PMMA denture surface is susceptible to adhesion and colonization of microorganisms, which can survive for a long time and cause various oral diseases. Therefore, it's crucial to enhance the antimicrobial activity of PMMA. In this study, the ZnO/GO composites not only significantly improved the mechanical properties of PMMA but also endowed the PMMA with an antibacterial effect. In addition, there was no significant difference in antibacterial effect of the aged and the non-aged modified resin, indicating that the ZnO/GO modified resin can still maintain good antimicrobial properties after a long period of use. Figure 7 shows the antibacterial mechanism of the modified resin. The antimicrobial activity of ZnO/GO nanocomposites mainly relies on the continuous release of Zn^{2+} and the production of ROS [20] [21]. In addition, the sharp edges of GO nanosheets exerting membrane stress effect possess the ability to

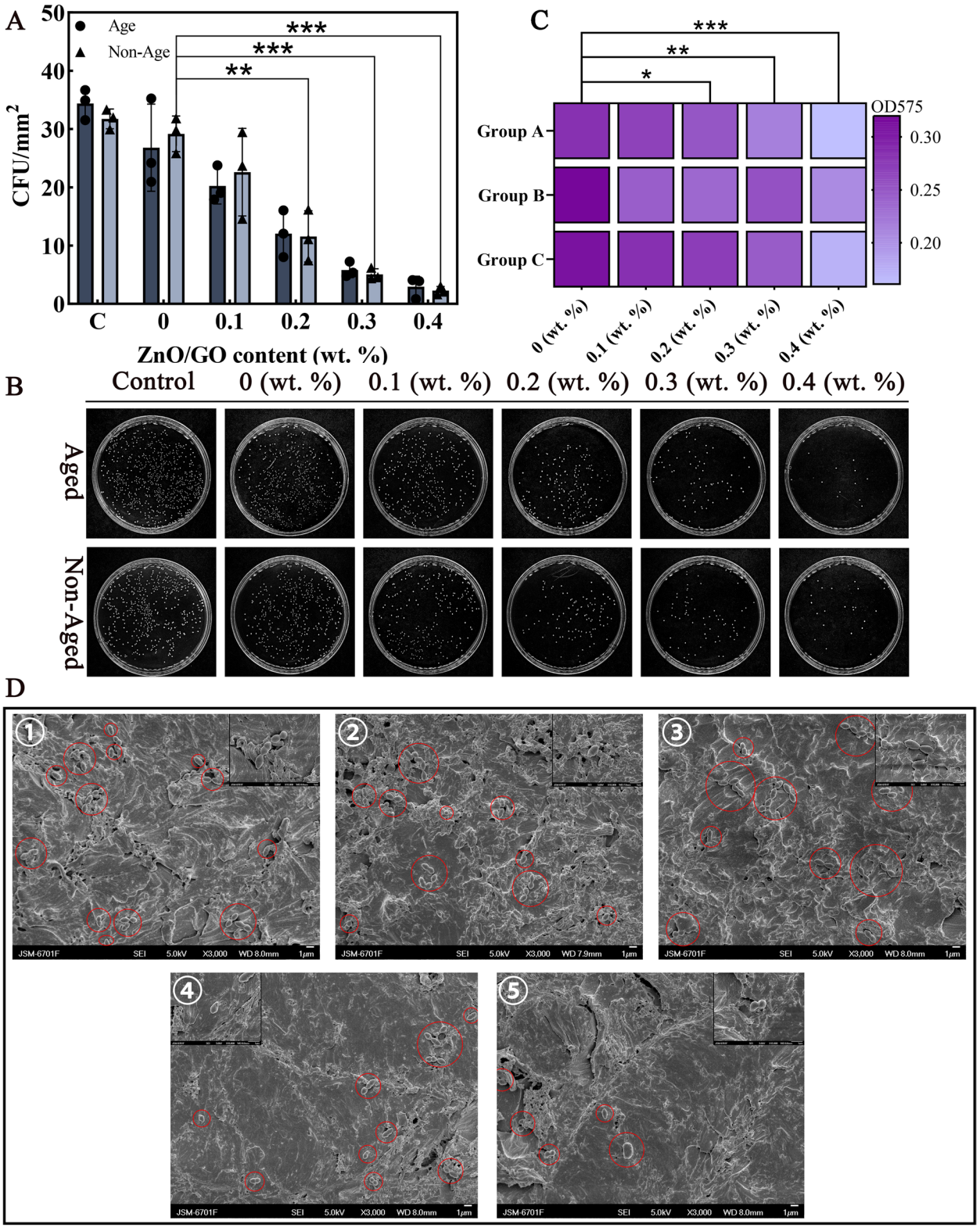

Fig. 5 Surface bacterial count (**A**), Plate count (**B**) and absorbance of crystal violet staining for surface biofilm (**C**) of the modified PMMA, SEM images of surface bacteria on the modified PMMA (D, ①-⑤ show the 0 wt.%, 0.1 wt.%, 0.2 wt.%, 0.3 wt.% and 0.4 wt.% of ZnO/GO respectively) ($n=3$, * $p<0.05$, ** $p<0.01$, *** $p<0.001$). CFU, colony-forming units

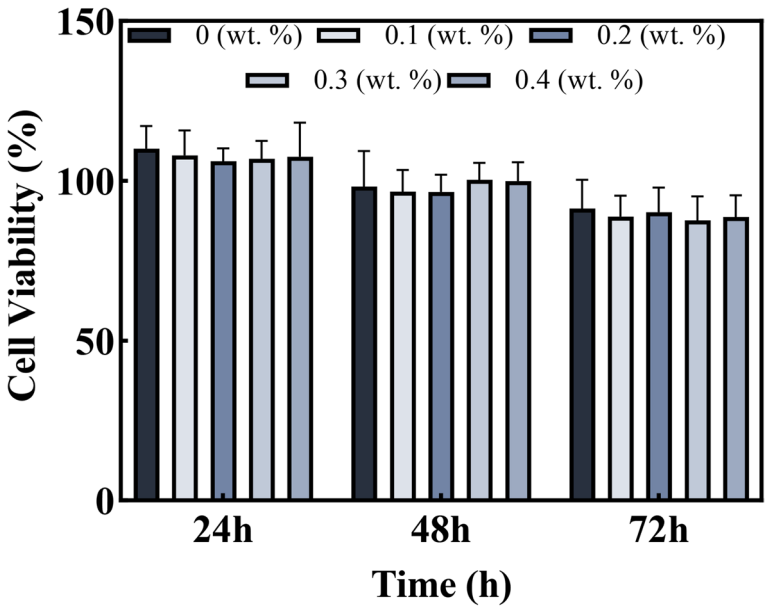

Fig. 6 Cell viability of the modified PMMA

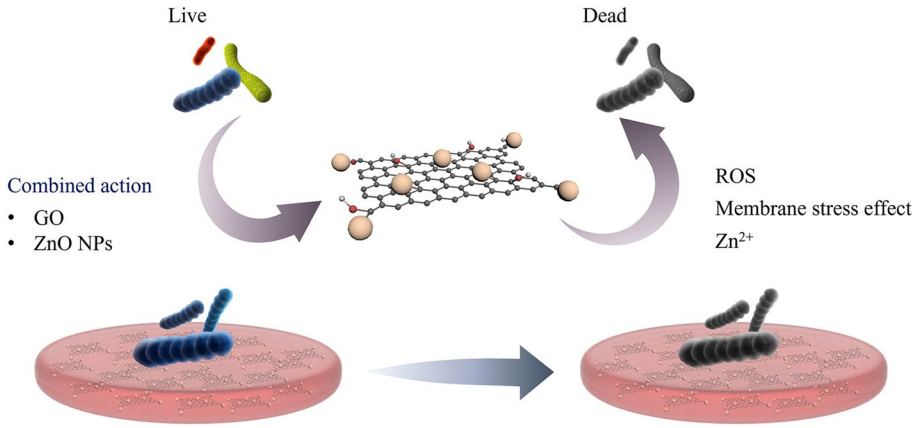

Fig. 7 Schematic diagram of antibacterial mechanism of the modified PMMA. ROS, reactive oxygen species

inflict physical harm to the bacterial membrane, resulting in the leakage of intracellular matrix, which ultimately leading to the inactivation of bacteria [41].

No cytotoxicity is an important basis for the PMMA applications in the oral. Although it had been shown that the cell viability decreases slightly with time after the treatment of L929 cells with modified resins leachate, there was no statistical difference among control groups and experimental groups at 24, 48, and 72 h, which indicated that the modified PMMA had no cytotoxicity. This is due to the excellent biocompatibility of ZnO/GO nanocomposites.

Conclusions

In this paper, ZnO/GO nanocomposites were successfully constructed using ZnO nanoparticles and GO sheets, and introduced into PMMA resin. Moreover, PMMA showed superior physical, mechanical and antibacterial activity after modification by ZnO/GO nanocomposites. Cytotoxicity evaluation also showed that the addition of ZnO/GO nanocomposites had no effect on the cytotoxicity of PMMA, confirming its safety in oral. This study opens up a new way for the antibacterial application of nanotechnology in oral materials, and is expected to become an ideal material for prosthodontics.

Abbreviations

PMMA	Polymethyl Methacrylate
ZnO/GO	Zinc oxide/Graphene oxide
ROS	Reactive Oxygen Species
TEM	Transmission Electron Microscopy
XRD	X-ray Diffractometer
FTIR	Fourier Transform Infrared
ISO	International Standard Organization
SEM	Scanning Electron Microscopy
LB	Luria-Bertani
CFU	Colony-Forming Unit
PBS	Phosphate Buffer Saline
DMEM	Dulbecco's Modified Eagle Medium
FBS Fetal	Bovine Serum
RGO	Reduced Graphene Oxide

Acknowledgements
Not applicable.

Authors' contributions
Shaofan Ruan designed this study and wrote the manuscript. Liling Ren and Rui Chen provided the funding support for this research, supervising and revising the manuscript. Shaofan Ruan, Yanzong Zhao, Jie Ma, Yian Guan and Jianqiang Ma contributed to the experiments and data analysis.

Funding
This work was supported by Gansu Province Key Lab of Maxillofacial Reconstruction and Intelligent Manufacturing (Grant No. ZDKF20210102) and Hospital of Stomatology Lanzhou University Scientific Research Project (Grant Nos. lzukqky2022-p05, lzukqky-2022-q01).

Availability of data and materials
The results of data extraction in this study are available from the corresponding author on reasonable request.

Declarations

Ethics approval and consent to participate
Not applicable.

Consent for publication
Not applicable.

Competing interests
The authors declare no competing interests.

Received: 10 May 2024 Accepted: 14 August 2024
Published online: 29 August 2024

References

1. Alp G, Johnston WM, Yilmaz B. Optical properties and surface roughness of prepolymerized poly(methyl methacrylate) denture base materials. J Prosthet Dent. 2019;121:347–52.
2. Ruse ND, Sadoun MJ. Resin-composite blocks for dental CAD/CAM applications. J Dent Res. 2014;93:1232–4.
3. Ghaffari T, Hamedirad F, Ezzati B. In Vitro Comparison of Compressive and Tensile Strengths ofAcrylic Resins Reinforced by Silver Nanoparticles at 2% and 0.2% Concentrations. J Dent Res Dent Clin Dent Prospects. 2014;8:204–9.
4. Matsuo H, Suenaga H, Takahashi M, Suzuki O, Sasaki K, Takahashi N. Deterioration of polymethyl methacrylate dentures in the oral cavity. Dent Mater J. 2015;34:234–9.
5. Walczak K, Schierz G, Basche S, Petto C, Boening K, Wieckiewicz M. Antifungal and Surface Properties of Chitosan-Salts Modified PMMA Denture Base Material. Molecules. 2020;25:5899.
6. Peng X, Cheng L, You Y, Tang C, Ren B, Li Y, et al. Oral microbiota in human systematic diseases. Int J Oral Sci. 2022;14:1–11.
7. Gleiznys A, Zdanavičienė E, Žilinskas J. Candida albicans importance to denture wearers. A literature review Stomatologija. 2015;17:54–66.
8. Diamanti-Kipioti A, Gusberti FA, Lang NP. Clinical and microbiological effects of fixed orthodontic appliances. J Clin Periodontol. 1987;14:326–33.
9. Chang HS, Walsh LJ, Freer TJ. The effect of orthodontic treatment on salivary flow, pH, buffer capacity, and levels of mutans streptococci and lactobacilli. Aust Orthod J. 1999;15:229–34.
10. Li X, Kolltveit KM, Tronstad L, Olsen I. Systemic Diseases Caused by Oral Infection. Clin Microbiol Rev. 2000;13:547–58.
11. Cruz PC, de Andrade IM, Peracini A, de Souza-Gugelmin MCM, Silva-Lovato CH, de Souza RF, et al. The effectiveness of chemical denture cleansers and ultrasonic device in biofilm removal from complete dentures. J Appl Oral Sci Rev FOB. 2011;19:668–73.
12. Sesma N, Rocha AL, Laganá DC, Costa B, Morimoto S. Effectiveness of denture cleanser associated with microwave disinfection and brushing of complete dentures: in vivo study. Braz Dent J. 2013;24:357–61.
13. Zore A, Abram A, Učakar A, Godina I, Rojko F, Štukelj R, et al. Antibacterial Effect of Polymethyl Methacrylate Resin Base Containing TiO2 Nanoparticles. Coatings. 2022;12:1757.
14. Fathima Y, Sampathkumar J, Ramakrishnan H, Azhagarasan NS. Evaluation of the effect of EDTA on the antifungal properties, flexural strength, and colour stability of heat polymerised PMMA resin for implant overdentures. 2022;41:15–24.
15. Zhou W, Zhao H, Li Z, Huang X. Autopolymerizing acrylic repair resin containing low concentration of dimethylaminohexadecyl methacrylate to combat saliva-derived bacteria. J Mater Sci Mater Med. 2022;33:49.
16. Marić I, Zore A, Rojko F, Škapin AS, Štukelj R, Učakar A, et al. Antifungal Effect of Polymethyl Methacrylate Resin Base with Embedded Au Nanoparticles. Nanomater Basel Switz. 2023;13:2128.
17. Tijana A, Valentina V, Natasa T, Milos H-M, Suzana GA, Milica B, et al. Mechanical properties of new denture base material modified with gold nanoparticles. J Prosthodont Res. 2021;65:155–61.
18. Sun J, Wang L, Wang J, Li Y, Zhou X, Guo X, et al. Characterization and evaluation of a novel silver nanoparticles-loaded polymethyl methacrylate denture base: In vitro and in vivo animal study. Dent Mater J. 2021;40:1100–8.
19. Zhou G, Li Y, Xiao W, Zhang L, Zuo Y, Xue J, et al. Synthesis, characterization, and antibacterial activities of a novel nanohydroxyapatite/zinc oxide complex. J Biomed Mater Res A. 2008;85:929–37.
20. Dwivedi S, Wahab R, Khan F, Mishra YK, Musarrat J, Al-Khedhairy AA. Reactive oxygen species mediated bacterial biofilm inhibition via zinc oxide nanoparticles and their statistical determination. PLoS ONE. 2014;9:e111289.
21. Sirelkhatim A, Mahmud S, Seeni A, Kaus NHM, Ann LC, Bakhori SKM, et al. Review on Zinc Oxide Nanoparticles: Antibacterial Activity and Toxicity Mechanism. Nano-Micro Lett. 2015;7:219–42.
22. Li Y, Zhang W, Niu J, Chen Y. Mechanism of photogenerated reactive oxygen species and correlation with the antibacterial properties of engineered metal-oxide nanoparticles. ACS Nano. 2012;6:5164–73.
23. Wang Y-W, Cao A, Jiang Y, Zhang X, Liu J-H, Liu Y, et al. Superior Antibacterial Activity of Zinc Oxide/Graphene Oxide Composites Originating from High Zinc Concentration Localized around Bacteria. ACS Appl Mater Interfaces. 2014;6:2791–8.
24. Xu C, Wang X, Yang L, Wu Y. Fabrication of a graphene-cuprous oxide composite. J SOLID STATE Chem. 2009;182:2486–90.
25. Yang J, Zhao J-J, Han C-R, Duan J-F. Keys to enhancing mechanical properties of silica nanoparticle composites hydrogels: The role of network structure and interfacial interactions. Compos Sci Technol. 2014;95:1–7.
26. Vozniak I, Zaïri F, Hosseinnezhad R, Morawiec J, Galeski A. Design of hybrid PLA/PBS/POM composite based on In-Situ formation of interpenetrating fiber networks. Compos Part Appl Sci Manuf. 2021;151: 106667.
27. Cahyanto A, Martins MVS, Bianchi O, Sudhakaran DP, Sililkas N, Echeverrigaray SG, et al. Graphene oxide increases PMMA's resistance to fatigue and strength degradation. Dent Mater. 2023;39:763–9.
28. Han Y, Hao L, Zhang X. Preparation and electrochemical performances of graphite oxide/polypyrrole composites. Synth Met. 2010;160:2336–40.

29. Szabó T, Berkesi O, Forgó P, Josepovits K, Sanakis Y, Petridis D, et al. Evolution of Surface Functional Groups in a Series of Progressively Oxidized Graphite Oxides. Chem Mater. 2006;18:2740–9.
30. Si Y, Samulski ET. Synthesis of water soluble graphene. Nano Lett. 2008;8:1679–82.
31. Berli C, Thieringer FM, Sharma N, Müller JA, Dedem P, Fischer J, et al. Comparing the mechanical properties of pressed, milled, and 3D-printed resins for occlusal devices. J Prosthet Dent. 2020;124:780–6.
32. Figuerôa RMS, Conterno B, Arrais CAG, Sugio CYC, Urban VM, Neppelenbroek KH. Porosity, water sorption and solubility of denture base acrylic resins polymerized conventionally or in microwave. J Appl Oral Sci Rev FOB. 2018;26:e20170383.
33. Cahyanto A, Martins MVS, Bianchi O, Sudhakaran DP, Sililkas N, Echeverrigaray SG, et al. Graphene oxide increases PMMA's resistance to fatigue and strength degradation. Dent Mater Off Publ Acad Dent Mater. 2023;39:763–9.
34. Paz E, Forriol F, Del Real JC, Dunne N. Graphene oxide versus graphene for optimisation of PMMA bone cement for orthopaedic applications. Mater Sci Eng C Mater Biol Appl. 2017;77:1003–11.
35. Delaviz Y, Finer Y, Santerre JP. Biodegradation of resin composites and adhesives by oral bacteria and saliva: a rationale for new material designs that consider the clinical environment and treatment challenges. Dent Mater Off Publ Acad Dent Mater. 2014;30:16–32.
36. Giti R, Firouzmandi M, Zare Khafri N, Ansarifard E. Influence of different concentrations of titanium dioxide and copper oxide nanoparticles on water sorption and solubility of heat-cured PMMA denture base resin. Clin Exp Dent Res. 2022;8:287–93.
37. Goncalves G, Marques PAAP, Barros-Timmons A, Bdkin I, Singh MK, Emami N, et al. Graphene oxide modified with PMMA via ATRP as a reinforcement filler. J Mater Chem. 2010;20:9927–34.
38. Darvell BW, Murray MD. Complete denture retention. Part I: Physical analysis of the mechanism. Hysteresis of the solid-liquid contact angle. J Prosthet Dent. 1990;64:507–8.
39. Cierech M, Osica I, Kolenda A, Wojnarowicz J, Szmigiel D, Lojkowski W, et al. Mechanical and Physicochemical Properties of Newly Formed ZnO-PMMA Nanocomposites for Denture Bases. Nanomaterials. 2018;8:305.
40. Lazarin AA, Machado AL, Zamperini CA, Wady AF, Palomari Spolidorio DM, Vergani CE. Effect of experimental photopolymerized coatings on the hydrophobicity of a denture base acrylic resin and on Candida albicans adhesion. Arch ORAL Biol. 2013;58:1–9.
41. Shi L, Chen J, Teng L, Wang L, Zhu G, Liu S, et al. The Antibacterial Applications of Graphene and Its Derivatives. Small Weinh Bergstr Ger. 2016;12:4165–84.

Publisher's Note